Hypervelocity Impact Test Fragment Modeling: Modifications to the Fragment Rotation Analysis and Lightcurve Code

Michael F. Gouge[1]

Hypervelocity impact tests on test satellites are performed by members of the orbital debris scientific community in order to understand and typify the on-orbit collision breakup process. By analysis of these test satellite fragments, the fragment size and mass distributions are derived and incorporated into various orbital debris models. These same fragments are currently being put to new use using emerging technologies. Digital models of these fragments are created using a laser scanner. A group of computer programs referred to as the Fragment Rotation Analysis and Lightcurve code uses these digital representations in a multitude of ways that describe, measure, and model on-orbit fragments and fragment behavior. The Dynamic Rotation subroutine generates all of the possible reflected intensities from a scanned fragment as if it were observed to rotate dynamically while in orbit about the Earth. This calls an additional subroutine that graphically displays the intensities and the resulting frequency of those intensities as a range of solar phase angles in a Probability Density Function plot. This document reports the additions and modifications to the subset of the Fragment Rotation Analysis and Lightcurve concerned with the Dynamic Rotation and Probability Density Function plotting subroutines.

Nomenclature

A/m = Area to Mass Ratio
CCD = Charge-Coupled Device
FRAL = Fragment Rotation Analysis and Lightcurve code
$\vec{F}$ = Field Vector
GEO = Geosynchronous Earth Orbit
JSC = Johnson Space Center
Lc = Characteristic Length
$\hat{n}$ = Surface Normal
ODPO = Orbital Debris Program Office
NASA = National Aeronautics and Space Administration
PDF = Probability Density Function
SEM = Size Estimation Model
SPA = Solar Phase Angle
UN = United Nations
3D = Three dimensional

I. Introduction

The NASA Orbital Debris Program Office (ODPO) uses data from radar and optical observations to track and characterize orbital debris to help fulfill a mission to define the Orbital Debris (OD) environment. This information allows for more than 20,000 pieces of orbital debris to be tracked and catalogued. One advantage of telescopic observation is that more detailed information about the individual debris pieces may be discovered by performing photometric analysis, in particular lightcurve generation. This process, involving tracking and recording the reflected light intensities from a single object over a period of time, can yield approximations of size, shape, and possibly the area-to-mass ratio (A/m). However, in order to attribute these properties to orbital debris with certainty, a similar analysis must be performed in a laboratory. This research is vital as the science of interpreting telescopic

[1]TSGC Intern, Orbital Debris Program Office, Johnson Space Center, University of Texas at San Antonio

data is still in its nascency. Laboratory analysis provides an understanding of reflectance behavior for known objects under controlled conditions. This in turn, affords a comparison of photometric observations of known, terrestrially tested debris objects and data for observed orbital debris and justifies our attribution of these various physical properties to objects that appear as nothing more than glints of light in the sky.

Presently, a little more than half of the orbital debris population is comprised of fragmentation debris. To better understand this dominant portion of the orbital debris environment, hypervelocity satellite impact tests are performed terrestrially in conditions approximating those found in Earth's orbit. These fragments undergo the photometric analysis mentioned above. This laboratory work is time intensive and requires phenomenal expertise. To alleviate this time constraint the ODPO created a system to produce three-dimensional (3D) computer scans of test fragments that allow a 3D digital representation to perform this photometric analysis. This makes it possible to produce whole ranges of lightcurves in a small fraction of the time it takes to create a single lightcurve by hand. A 3D laser scanner creates digital models of test fragments. These 3D models are then used by the Fragment Rotation Analysis and Lightcurve code (FRAL). This code is a family of programs that among other things, seeks to model the lightcurve generation process. The Dynamic Rotation portion of this code generates the possible intensities of the scanned test fragment as if it were tumbling in space while orbiting Earth. A subroutine of this program then produces a probability density function (PDF) from this data. This paper will describe the function of this dynamic rotational program and related programs and subfunctions, relate their usefulness in the characterization of orbital debris, and explain recent modifications to the FRAL.

II. Orbital Debris

Orbital debris is classically defined as any human-made object in an Earth orbit that no longer serves a useful purpose. Since the dawn of the space age with the launch of Sputnik in 1957, thousands of such objects have been abandoned in orbit. Orbital debris consists of: spent rocket-bodies, non-functioning satellites, mission related debris (dropped tools and waste), sodium-potassium droplets (from Russian nuclear-powered satellites), and fragmentation debris.[1] The history of the orbital debris population is shown in Fig. 1.

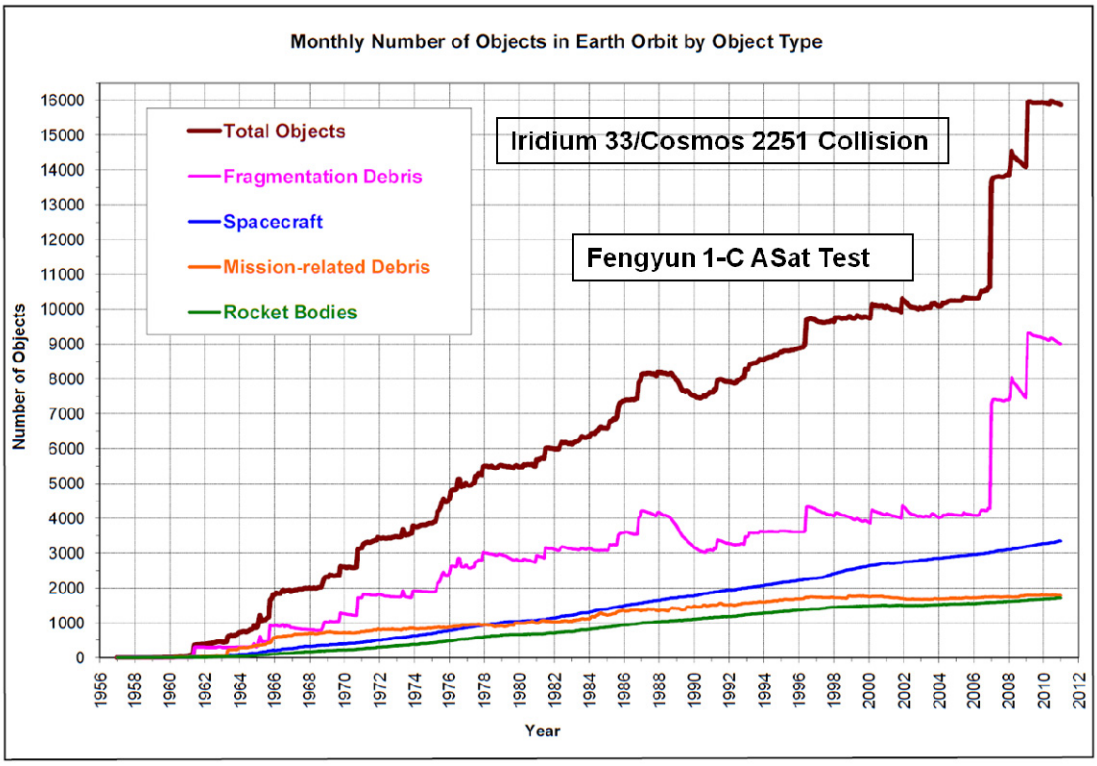

Figure 1. Number of objects in orbit by object type.[1]

Figure 1 shows that fragmentation debris accounts for roughly half of all debris objects currently in Earth's orbit. Furthermore, the growth of fragmentation debris is not a function of the number of missions executed but is driven by fragmentation events.

The mean velocity of objects in Low Earth Orbit (LEO) is approximately 7 km/s while that in Geosynchronous Earth Orbit (GEO) is 3 km/s. At these velocities, a piece of debris with negligible mass, like a paint flake, possesses enough momentum to cause catastrophic failure if it were to impact an unshielded satellite. The orbital debris population is and will continue to be dominated by fragments and fragmentation processes. Thus the ODPO attempts to measure and model fragmentation events and fragmentation debris to describe and predict the evolution of the orbital debris population.

A. Fragments and Fragmentation Processes

Orbital debris fragments are generally produced in one of three ways: anomalous events, explosions, and collisions. Anomalous events are generally minor in nature and produce small numbers of debris. These events are atypical by nature. They sometimes occur due to the decay of orbiting bodies: parts separating suddenly or paint flakes sloughing off a space-borne body. Explosions may be accidental or intentional. Unintentional explosions are generally attributed to the chemical reaction of stored energy left in a non-functioning orbiting body, such as rocket fuel or batteries. NASA and the UN have put international standards in place that require all future satellites and space vehicles to be purged of such energy sources before they may be abandoned. Intentional explosions include satellite self-destruction.

Collisions may occur between two fragments, two functioning orbiting bodies, a fragment and a functioning orbiting body, or as part of an anti-satellite-missile test. Collision events are predicted to drive the future growth of the orbital debris population (as they have the last 3 years, as seen in Fig. 1 above) as more and more debris are produced. To better understand the collision process and resulting satellite break-ups, scientists in the orbital debris community have labored to realistically reproduce the fragment-satellite collisions in laboratories across the world.

B. Hypervelocity Impact Tests

Several satellite fragmentation tests have been executed in the past few decades. Each has attempted to create on Earth a collision similar to what would occur in orbit. Thus, all of these various tests are performed in vacuum chambers using space-ready or micro satellites shot with small aluminum spheres, at both low and hypervelocities. The purpose of these tests is to determine the distribution of fragments by size, shape, mass, material, velocity, and the resulting area-to-mass ratios (A/m). These factors determine the behavior of the debris on-orbit, the rate of orbital decay, and reentry properties. Such tests led to the development of the NASA Standard Break-Up Model, which is an internationally accepted tool for describing on-orbit fragmentation distributions.

The ODPO preferred definition of debris size, characteristic length (Lc), attempts to model size in a way consistent with what would be observed via RADAR or telescopic observation. This length is developed by the following procedure[2]:

1) The absolute maximum distance between any two points on the object is called x.
2) The absolute maximum distance between any two points that could be projected onto a plane orthogonal to the x dimension is defined as y (see Fig. 2).
3) The longest projection dimension orthogonal to both x and y is defined as z.

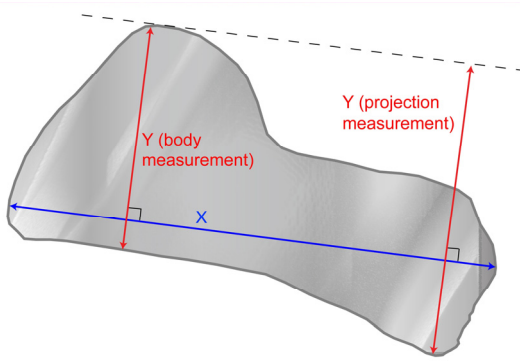

Figure 2. Lc measurement process.

An example of this measurement process, as performed in the meshing software, is shown in Fig. 3.

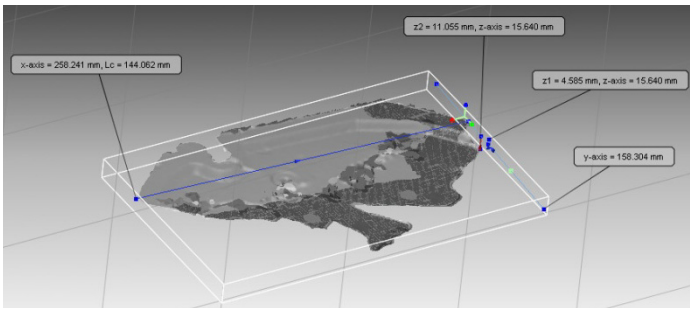

Figure 3. Lc measurement process example.

Lc is then defined as:

$$Lc = \frac{1}{3}(x + y + z)^{2} \qquad (1)$$

Breakup tests provide much useful data, including but not limited to size, mass, material and angular distributions of fragments. This data is used to predict the fragmentation behavior for future breakups. The A/m is of particular interest, as those objects with high A/m decay more quickly due to atmospheric drag and solar radiation pressure. In addition to taking size measurements, photometric analysis is performed in the ODPO Optical Measurement Center for the correlation of laboratory and telescopic measurements. This allows determination of shape, material, size, and, potentially, A/m for observed orbital debris fragments.[3]

III. Lightcurve Photometry

Photometry is the act of measuring light.[3] For light-curve photometry, one measures the intensity of light reflected by an object over time. The plot of intensity over time is a lightcurve. With a modern telescope fitted with a Charge-Coupled-Device (CCD), the measure of light intensity is found through the release of electrons of the photoelectric cell proportional to the amount of light that strikes its surface.[4] To create a descriptive representative light curve, the object's intensity should be plotted with respect to the solar phase angle instead of time.[3,4] The solar phase angle is defined as the angle between the line connecting the observer and the Sun and the line connecting the observer and the object, as seen in Fig. 4. An object will have a maximum intensity at 0°, as the light from the sun is reflected from the object surface directly to the observer. As the solar phase angle increases, the measure of reflected light intensity will decrease, until it reaches its nadir at 180°, at which point the reflected light intensity is effectively zero (as no sunlight is incident upon any face oriented towards the observer). From this point, the intensity will generally increase until it reaches a maximum at the 0° solar phase angle.[4]

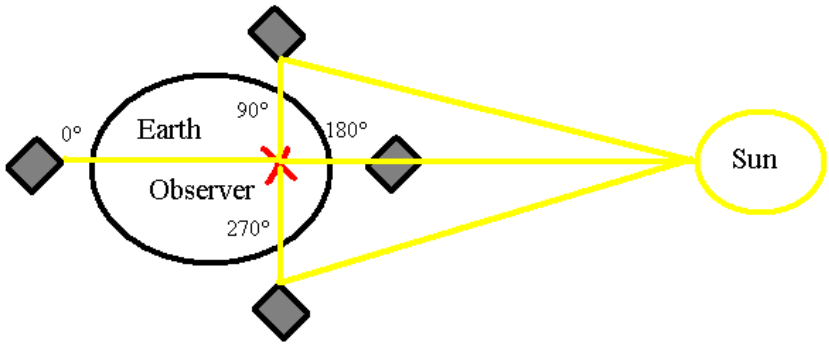

Figure 4 Solar phase angle.

Photometric phase functions are mathematical models used to predict the reflected intensity of a body in space.[3] There are three classical phase functions, Specular, Lunar, and Lambertian, along with two hybrid combinations thereof, Specular-Lambertian and Lambertian-Lunar.[5] Specular reflections are simply mirror like reflections that spread evenly into space, independent of solar phase angle. This is modeled mathematically as:

$$Specular\ Intensity = \frac{1}{4\pi}^{5} \qquad (2)$$

Lunar reflections *are* dependent upon solar phase angle (SPA). The moon disperses reflected light unevenly due to its rough and multifarious surface features.[3] An empirical function for the reflected intensity was developed, which is:

$$Lunar\ Intensity = \frac{5}{\pi^2} \cdot 5.3095 \cdot 10^{-5} \cdot SPA^2 - 1.2591 \cdot 10^{-2} \cdot SPA + .79121\ 6 \quad (3)$$

The Lambertian phase function models an object that is perfectly diffuse. Lambertian intensities may be found for a range of solar phase angles using the following equation:

$$Lambertian\ Intensity = \frac{2}{3\pi^2}(sin(SPA) + (\pi - SPA) \cdot cos(SPA))^{5} \quad (4)$$

The hybrid Specular-Lambertian phase function is simply a mixture of its two component functions:

$$Specular - Lambertian\ Intensity = \beta \cdot Specular\ Intensity + (1 - \beta) \cdot Lambertian\ Intensity^{5} \quad (5)$$

Where the term β is the percent of mixing, which is generally calculated using 10% step increments. Similarly, the Lambertian-Lunar Intensity may be found using:

$$Lambertian - Lunar\ Intensity = \beta \cdot Lambertian\ Intensity + (1 - \beta) \cdot Lunar\ Intensity^{5} \quad (6)$$

Each of these functions is plotted in Fig. 5: If the surface characteristics of an object (namely color and material) are known, it is possible to compare its lightcurve with that of another object with the same surface. Surface characterization may be accomplished via spectroscopy or color-filter photometry.[3] Object size may be determined via the new optical size estimation model (SEM) currently in development.

The SEM is based upon total albedo (A), magnitude of the light intensity from the sun (Msun), the magnitude of the light intensity reflected by the object (Mobs), the phase function, and altitude(R). Based on empirical observations, space debris is best modeled using the purely Lambertian phase function.[3]

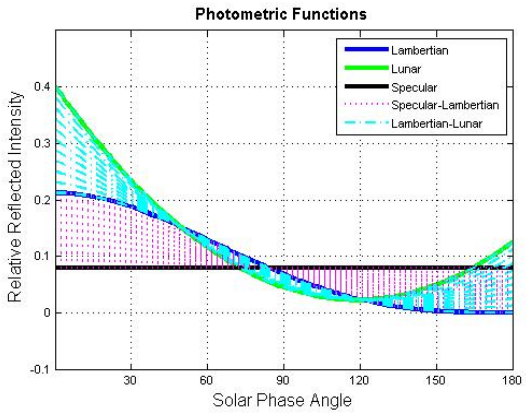

Figure 5. Plot of the photometric functions.

The equation for size is then:

$$Lc = \frac{2 \cdot R}{(\pi \cdot A \cdot Lambertian\ Intensity)^{-0.5}} \cdot 10^{\left(\frac{Mobs(R) + Msun(R)}{-5.0}\right)^{5}} \quad (7)$$

Two objects of simple shape (sphere, plate, or cuboid) with well-matching lightcurves, surface properties, and size, have the same shape.[3] Thus one can use laboratory lightcurves in conjunction with lightcurves from on orbit fragments to typify the shapes of observable orbital debris.

Knowing the size and shape of the debris fragment, one can calculate an approximate mean cross sectional-area, based on the equations developed in the NASA Standard Breakup Model. These equations for plate-like and irregularly shaped objects are tabulated below:

$$Plate\ Mean\ Cross\ Sectional\ Area = \frac{1}{2}(Lc^2 + 2Lc * z)\ ^{7} \quad (9)$$

$$Irregular\ Mean\ Cross\ Sectional\ Area = \frac{\pi}{12}(x \cdot y + y \cdot z + x \cdot z)\ ^{7} \quad (10)$$

If it is possible, via the examination of the surface characteristics of the debris, to determine the material of the observed fragment, one may use an approximation of volume and known material density to determine object mass. With this mass one can immediately find an estimate for the A/m. Having determined these properties for a piece of orbital debris, it is possible to model the rate of the object's orbital decay.

IV. 3D Fragment Scanning

Digital models of hypervelocity test fragments are created using a handheld 3D scanner**.** This device and its corresponding software are capable of measuring objects down to approximately 1 mm. Once the object has been scanned, it is imported into the scan analysis program modeling environment. Using this software multiple scans of the same object may be merged, which is necessary to create a full model from scanning the various sides of an object. Erroneous facets may be deleted at this point, and small holes in the scanned surface may also be patched. The scan analysis program also allows for the characteristic length to be quickly determined, through the line drawing, measuring, and plane projection tools. Once this process has been completed, and the scan has been verified as representative of the physical test fragment, vertex and facet files are exported from the scan analysis program software. These two files together describe completely the three-dimensional geometry of the scanned fragment. It is the creation of this mathematical 3D data which allows for the digital modeling of the photometric process, along with the calculation of volume and average cross sectional area, amongst the myriad possible present and future uses.

V. The Dynamic Rotational Evolution Model

The ODPO decided to create and analyze 3D models of fragments to help improve the understanding of satellite fragmentation processes and satellite fragment properties. These models are used in various ways such as modeling, fragment analysis, and comparison with optical research. Furthermore, the 3D models preserve the satellite fragments in a digital form.

At the beginning of this particular project the FRAL code consisted of 157 separate programs and subroutines. However, only eight of those programs are used in the portion of the code investigated here, and only four of those eight were altered during this phase of the project. This is the portion of code that generates the frequency for a particular relative reflected intensity from the scanned test fragment that would be observed if the object was on orbit, as the phase angle changes for a dynamically rotating object. A set of brief program descriptions are presented below.

A. Initialization subroutine

The initialization subroutine is read by the dynamic rotation program. This subroutine inputs the vertices and facets files that are analyzed by the Dynamic Rotation Program. It sets the titles for all related graphical output programs. Furthermore, the initialization subroutine sets the number of random object orientations, the value of maximum intensity, and the number of phase angles considered.

B. Dynamic Rotation Program

This is the main program of the dynamic rotation analysis performed by the FRAL. This program loops through the solar phase angles and for each phase angle, generates thousands of random object orientations (in quaternion coordinates). The main program then references the angle and intensity generating subroutine. This subroutine calculates the angle between the sun and the object, the angle between the observer and the object, and then checks to see if the observer can see the object based on the prior angles.[8] If the object is within the observer's line of sight, the subroutine calculates the relative reflected specular and diffuse intensities. These intensities are returned by the subroutine to the main program loop, which records these intensities into two arrays, one for specular data and the other for diffuse data, for the phase angle currently considered.

C. PDF Plotting Subroutine

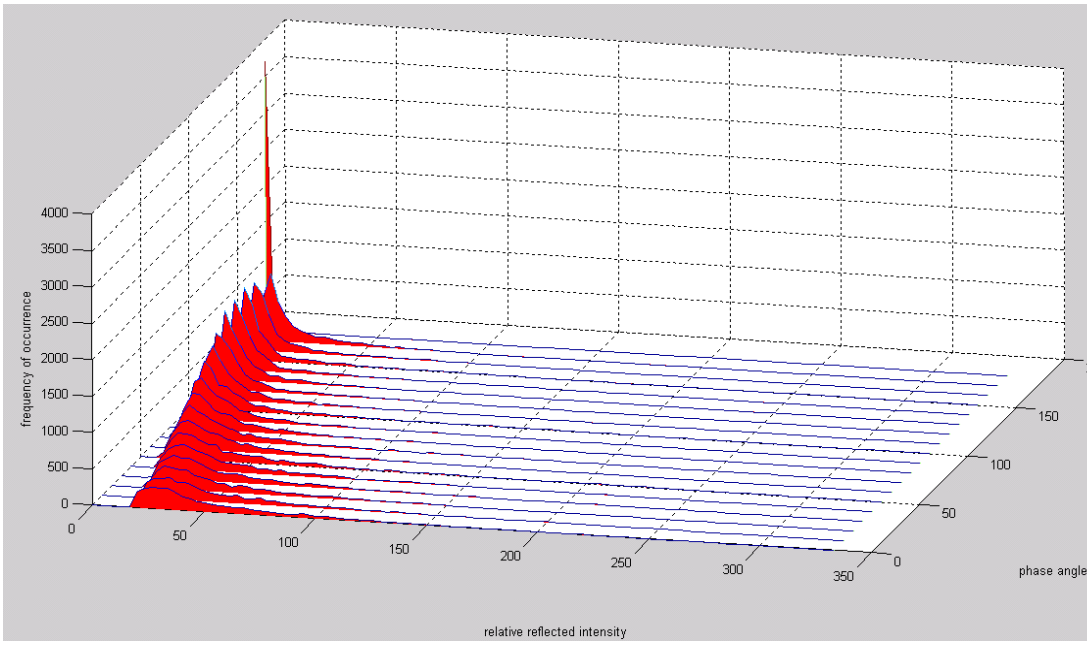

Figure 6 Original waterfall PDF plot of SOCIT4 252A1 large flake.

This is the plotting program that is run after the dynamic rotation program. The code creates a 3D graph of the Probability Density Function (PDF) from the two arrays mentioned above. This program assumes that total observed reflected light is 50% specular, 50% diffuse as established by laboratory photometry of test satellite fragments.[3] The plotting program creates a total combined intensity array from a mixture of the specular and diffuse intensity arrays. It then distributes the possible intensities in equal bins (equal to the number of phase angles) between the minimum and maximum intensities. The main program loop generates a frequency histogram from the intensities for each phase angle. These are recorded to an array of frequency of particular intensities at each phase angle. The program then plots the resulting array (which is the PDF). This graph may be seen in Fig. 6.

VI. Motivation for Altering the FRAL

A list of requested changes is presented below.

1) Rotate the PDF axes so that relative reflected intensity was on the z-axis, phase angle on the y-axis, and frequency of occurrence on the x-axis. This alteration was desired to make the PDF graph easier to read by orientating the axes in the manner commonly found in two dimensional lightcurves (intensity plotted against phase angle).
2) Plot phase angles from 0 to 360 degrees in the PDF subroutine. Reflectance is not perfectly symmetric for changing SPA, thus it was deemed necessary to see all 360 solar phase angles.
3) Plot at one degree phase angle increments in the PDF subroutine. This increase in precision was desired so as to eliminate any loss of data that might occur using a larger step size.
4) Integrate in-house code for determination of volume and cross sectional area of the fragment pieces. The purpose of translating this code into FRAL isto fully integrate all programs and subfunctions together. This will allow a user to run the entire FRAL once for a single fragment.

Various other improvements to the code were made, namely decreasing the program run time and increasing ease of use for future users. These secondary ends necessitated changes in the angle and intensity generating subroutine, and the creation of two new subroutines. Finally, a third new program was created via the translation of the existing in-house code. This program calculates the volume and cross sectional area of the scanned fragments from their vertex and facet files.

VII. The Final Purpose of the FRAL: Satellite Fragment Database

The ultimate end of this program is for every scanned test fragment to be analyzed by the FRAL, which has many purposes including but not limited to:

- Generate a figure of the PDF plot for each fragment
- Calculate volume for each fragment
- Calculate average cross sectional area for each fragment
- Allow fragment preservation by reducing future fragment handling and creating a permanently accessible 3D model
- Produce accurate 3D representation of each fragment
- Generate light curves using: uniaxial, random, and dynamic rotations
- Produce PDF plot

This data then will be incorporated to the existing Satellite Fragment Database, which includes for each fragment:

- Material Information
- Shape Class
- Hand Measurements
- Estimated Mean Cross Sectional Area
- Mass
- Weight
- A/m
- Density
- Digital-model measurements
- Object photos
- Scan analysis program model file
- Scan analysis program facet and vertex files
- Images exported from the scan analysis program showing fragment measurements

This database will then be the primary source for obtaining reliable measurements and data from hypervelocity impact testing. This work will be used in various ODPO fragmentation research and modeling projects.

VIII. Modifications to the Existing Code

A. Initialization Subroutine

The major changes to this subroutine were for increasing ease of use and for changing the plot to show a 360 degree phase angle rotation at one degree increments. Commands were also inserted to allow the user to graphically choose the source vertex and facet files. The graph title (used in the various plotting programs) is now automatically generated from the vertices file name.

B. Dynamic Rotation Program

This subroutine was altered in several ways to decrease program runtime.

C. Angle and Intensity Generating Subroutine

Constants set within the loop of this program were moved to the Dynamic Rotation Program, so they were only set once. This reduced the Dynamic Rotation program runtime by 3.5%.

D. Plotting Program

This program was almost entirely rewritten. The numeric frequency of occurrence was changed to display the frequency of occurrence of intensities as a percentage. The desired change of axes was not implemented, due to the available plotting techniques for dependent and independent variables. Three new subplots were added. All of the plots were made to include the 360 degree, one degree increment phase-angles. A further modification was the option to import data in other formats. This allows the preservation of the intensity array for plotting the data without requiring multiple runs of the intensity generating subroutine for a single fragment. Quadratic fit lines were added to two of the new subplots, which are described in detail below. The output of this program is shown in its entirety in Fig. 7. A description of each subplot may be found below.

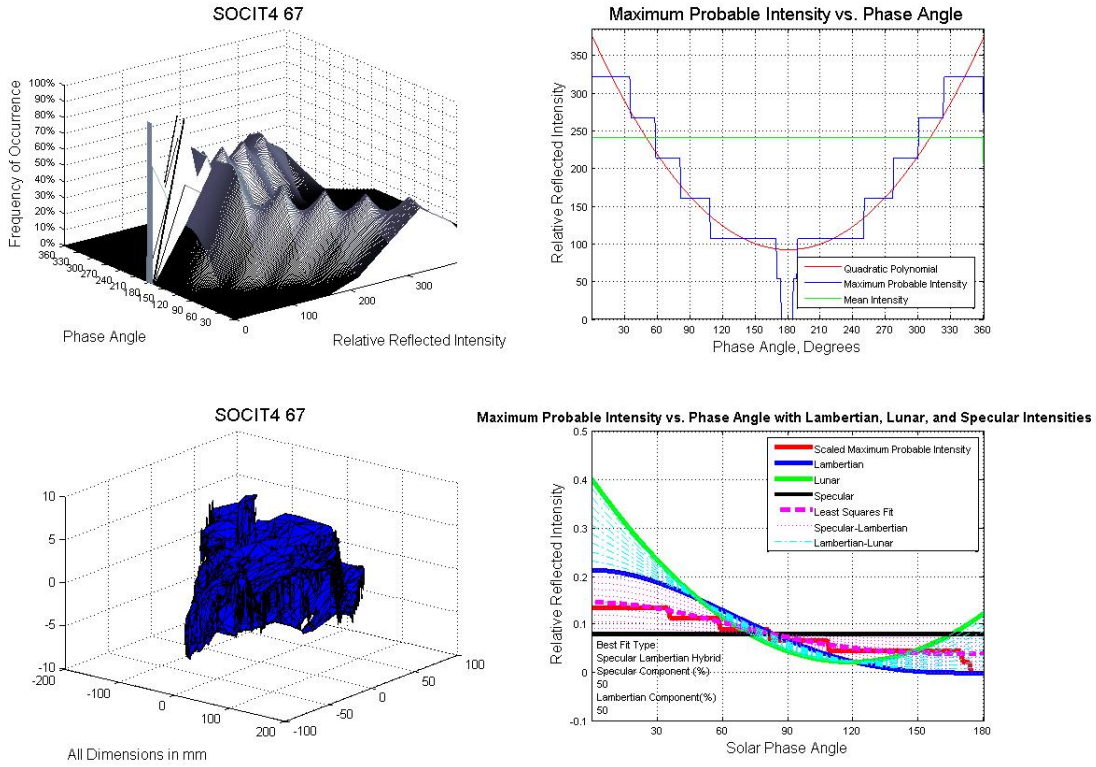

Figure 7. PDF subroutine plot.

E. 3D Render

Figure 8 shows the 3D rendering of the scanned fragment. It shows what the scanned object referenced by the PDF generator looks like for easy reference during analysis. This figure may be manipulated to see the object in different angles and finer detail.

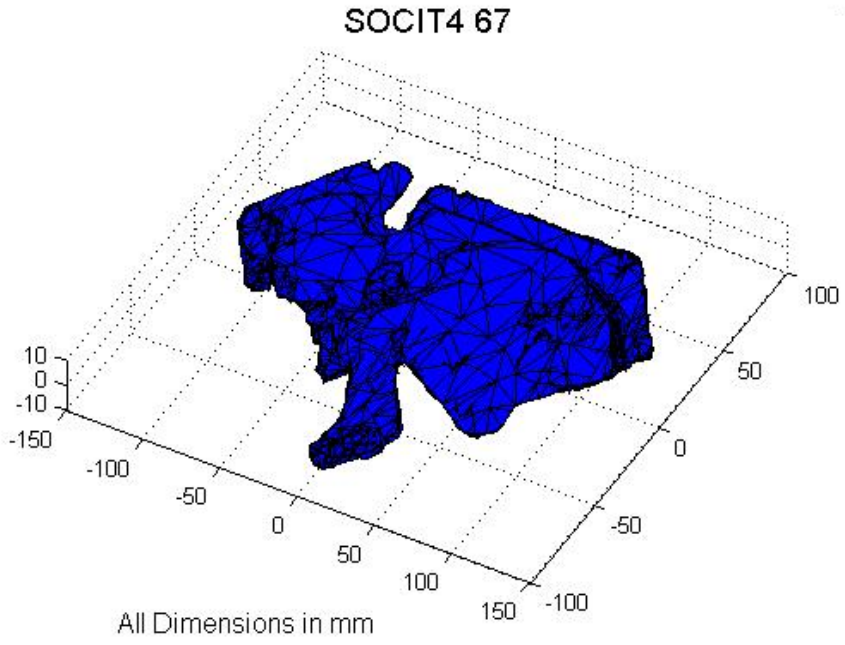

Figure 8. 3D render of test fragment.

F. Waterfall PDF Plot

Figure 9 is a waterfall plot of the PDF using the relative reflected intensity on the x-axis, the phase angle on the y-axis, and frequency of occurrence on the z-axis. One can immediately see the expected lightcurve behavior, intensity peaking at 0° and 360° solar phase angle and falling to zero at 180°. One can also read, from this graph, the relative likelihood of a certain intensity occurring at a certain phase angle.

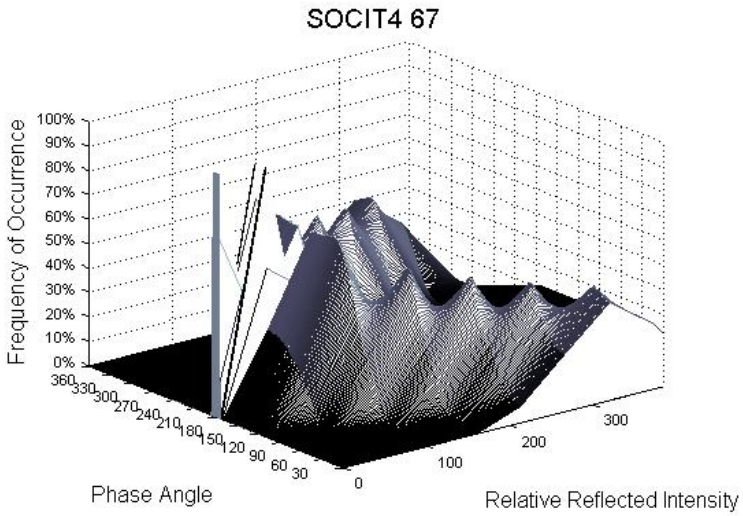

Figure 9. Waterfall PDF plot.

G. Maximum Probable Intensity vs. Phase Angle

Figure 10 shows the plot of the reflected intensity which is most likely to occur for each phase angle. These numbers are extracted from the same PDF data set. The green line (labeled Mean Intensity) represents the mean of all intensities. The blue line (labeled Maximum Probable Intensity) shows the intensities that occur with the highest frequency based on each considered phase angle. The red fit line (labeled Quadratic Polynomial) is a fit function used to create a smooth data set for this object, based on the maximum probable intensities.

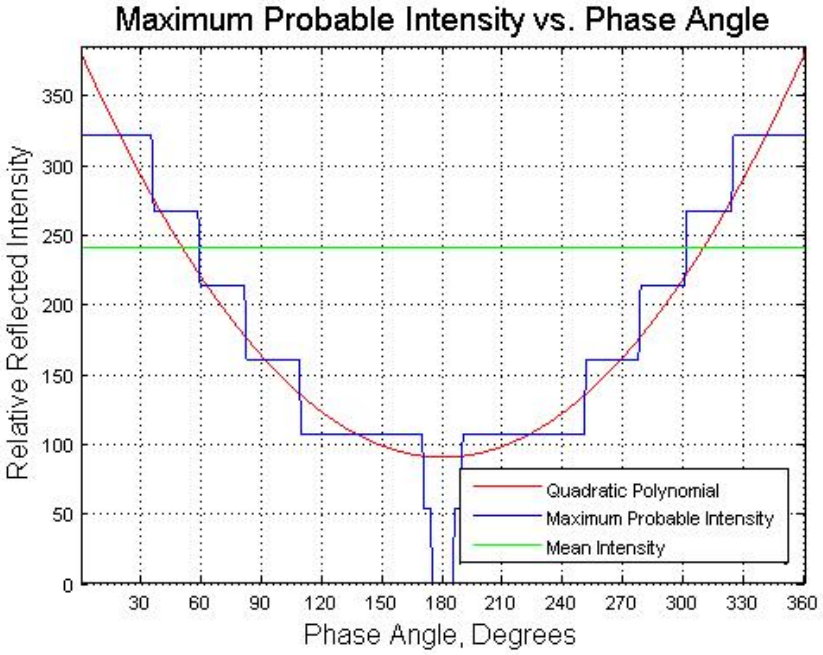

Figure 10. Maximum probable intensity as function of phase angle.

H. Maximum Probable Intensity vs. Phase Angle, with Lambertian, Lunar, and Specular Intensities

The graph seen in Fig. 11 allows for the direct comparison of the photometric behavior of the scanned fragment with the classical and hybrid light intensity functions described earlier in this paper. These functions are plotted along with the Maximum Probable Intensity line (described in section G above) and scaled to match the Lambertian line at 90°. Along with presenting a visual test of functional similitude, a numeric comparison between the scaled maximum probable intensity and each function is shown on the graph. This is achieved by using the least-squares method. The line with the lowest total R-value is chosen as the closest defining line, which is graphed in hot pink, and the associated best fit data (type, and if applicable, percentage of specular and diffuse components).

The PDF generation subroutine assumes that the object behaves in a Lambertian manner with 50% specular and 50% diffuse surface. This graph contradicts that assumption even though the data that creates this plot is generated using this contradicted assumption. However, there is a difference between the surface effect and the geometry effect on the overall light reflection of a fragment. The FRAL code treats all test fragments as aluminum (the most prevalent orbital debris material) and makes the assumptions just stated, *with respect to the object surface*. However, the geometry of the object influences how light will scatter from its surface. Objects that are large and flat will produce more specular flashes, while those with more rounded areas, or depressions, will scatter or capture incident light, which will not be recorded by an observer. Thus this graph helps with the interpretation of how the various geometrical features of test fragments will alter the lightcurves of different objects with identical surface characteristics.

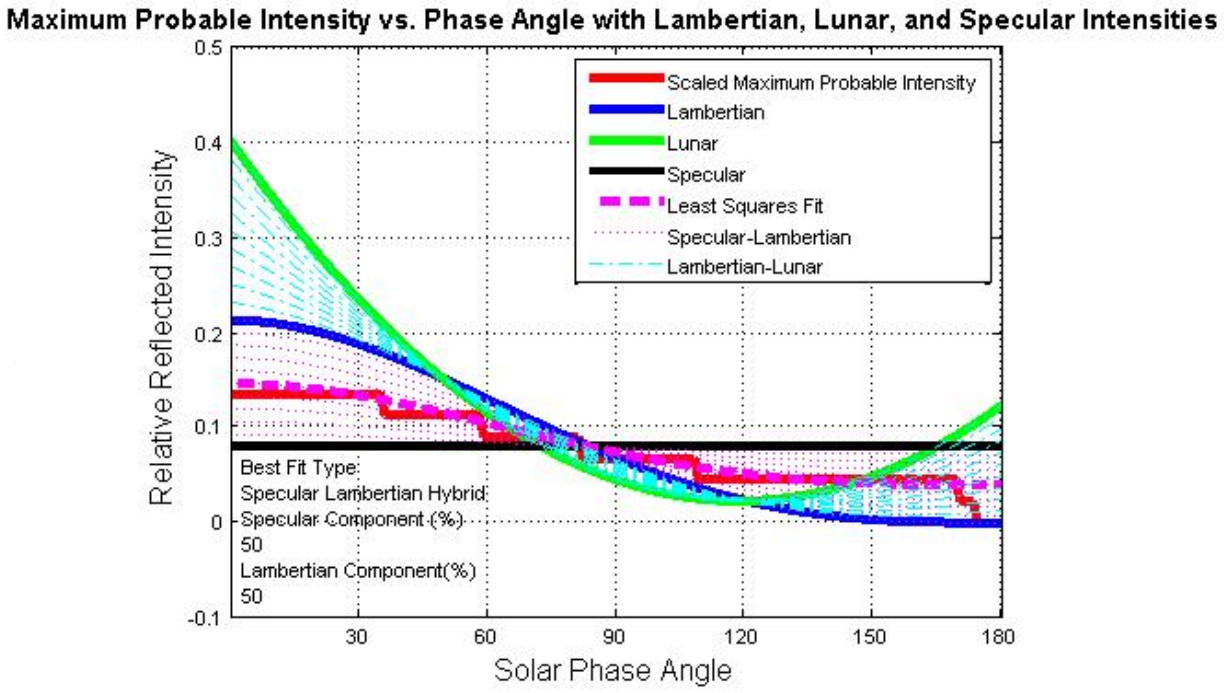

Figure 11. Comparison of scaled maximum probable intensity to standard photometric functions.

I. Facet Cleaning

A new program was created by the author of this document in order to eliminate the manual removal of unnecessary data in the exported scan analysis program facet files. These files in their raw state contain a text header along with the object vertex and facet data. The header and vertex data must be removed before they can be used by the initialization subroutine. In the past this was done by hand. In order to obviate the need for any such laborious file processing by users of FRAL, the facet cleaning program was created to take a raw facets file (using a graphical input), remove the header and vertices, and save the data to a file of the user's choice.

J. Volume and Mean Cross Sectional Area

Up to this point, the discussion of the FRAL code has focused upon the aspects concerning its Dynamic Rotation program. Looking at another standalone FRAL program, the focus is shifted to the terrestrial measurement of test satellite fragments. This code uses the same vertices and facets files from the 3D scanning process for an entirely different purpose. This program determines, through numeric integration, the volume and mean cross sectional area of a scanned fragment.

The primary reason to determine the volume and mean cross sectional area is because these properties affect the rate at which space-borne objects experience orbital decay. Orbital decay is caused primarily by gravitational perturbations, atmospheric drag and solar radiation pressure. Naturally objects with larger areas will experience larger total frictional forces as they travel through the atmosphere. Similarly, objects with larger surface areas will experience a greater total force from the solar radiation pressure. However, following Newton's Second Law, the orbital deceleration caused by these external forces is proportional to the measurement of inertia of the object, or its mass. Thus the loss of orbital velocity caused by these two forces is directly proportional to area and inversely proportional to mass. This is but one reason why the ODPO seeks to determine the area, area-to-mass ratio (A/m), and volume of orbital debris. These properties also affect the likelihood and energy of fragment collisions.

In addition, there is interest in using test fragment area calculations to validate the current RADAR size estimation model (SEM). This code computes volume and mean cross sectional area rapidly for hypervelocity impact test fragments, and allows all test fragment scan analysis codes integrated into a single meta-program to be run once for each fragment.

Volume is determined by Green's Function. Green's Function states that the volume (V) of an object may be calculated by integrating the dot product of the field vector ($\vec{F}$) with the surface normals ($\hat{n}$) over the entire surface (S), or:

$$\iiint \nabla \cdot \vec{F}\, dV = \iint \vec{F} \cdot \hat{n}\, dS \quad [9] \qquad (11)$$

To find the volume, the code first determines the surface normal of the facets. Then the centroid of the object is found. Next the field vector from the centroid and the facet location is determined. It then computes the dot product of the field vector and surface normal. Finally the results for all dot products are summed, yielding the object's volume.

Mean cross-sectional area is calculated in two distinct methods by this program, which allows for the validation of the two computational methods. The first method sums the facet areas observable from a set of random viewpoints. The second method uses the same random viewpoint, but projects the 3D object onto a gridded two-dimensional plane from this position, and sums the grid areas occupied by this object projection.

The first calculation method begins by generating a random viewpoint in polar coordinates and then creating a reference vector from this viewpoint. Then the program loops through the facets. For each facet the program first calculates the angle between the surface normal and the reference vector. Then, a logical test checks to see if the angle is less than 90°. If this is so, the facet is within view and it adds the area of the facet to the total area observed from the current viewpoint. Finally, the program sums and averages the viewpoint areas to find the mean cross sectional area from all the random viewpoints.

The second calculation method uses the same random viewpoint and reference vectors as in the first method. Yet it works by determining the area of the object as projected onto a two-dimensional plane, perpendicular to the reference vector. The plane is divided into equal areas creating a mathematical grid upon its surface (a visual representation of this process is seen in Fig. 12). The maximum and minimum bounds of the object projection within the grid are discovered. The program then projects each facet in turn upon the gridded area. The program searches through all of the grid sections to see if it is occupied by the facet in question, and if so, adds the area of the grid to the total area observable from the current viewpoint. Like the first method, the areas from all the viewpoints are summed and averaged to find the mean cross sectional area.

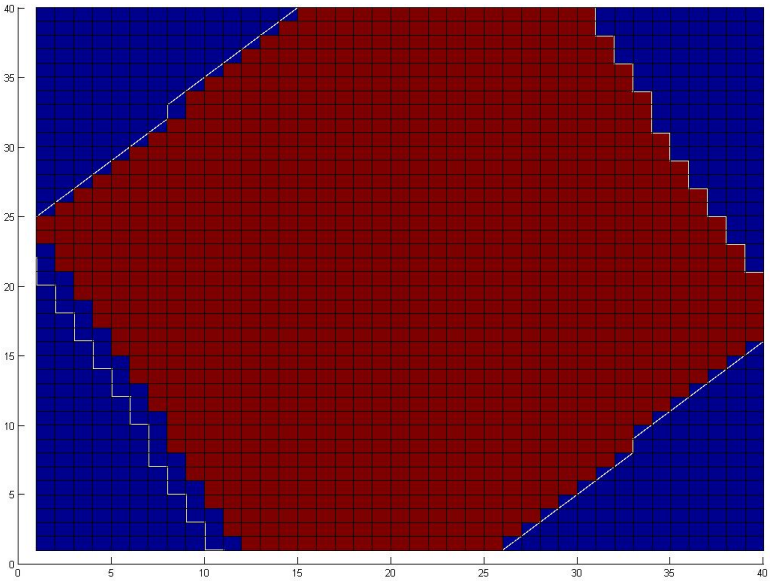

Figure 12. Projection of an object's cross sectional area onto a two-dimensional gridded surface, low resolution.

K. Integrated Program

It is a future goal of the ODPO to have a code that will perform a complete analysis of the scanned fragments and can be used by someone with minimal coding experience. This code allows such a user to run a single program, requiring no input beyond choosing the vertices and facets files (raw or processed) and typing in the title of the hypervelocity impact test. The rest of the program is automated to generate PDF data, save a figure of the PDF, and calculate the volume and mean cross-sectional area. In the future, it is desired that all other aspects of the FRAL be joined together by a similar program.

IX. Summary and Direction of Future Work

Over the course of this semester, the author has worked assiduously to transfer the mathematically elegant FRAL into a program with an equal elegance of ease-of-use and graphical output, while increasing the usefulness of the code. This has been achieved. In its current state the program may be run by a user unaware of its inner workings. The plotting program now displays three separate graphs that typify the object's photometric behavior according to needs of the ODPO end users. The graph that seeks to define the geometry-based photometric behavior will aid the development of astronomical science for orbital debris, which hitherto has not incorporated the effect of the geometry of debris objects when observing their reflected light intensities. Furthermore, the integration of the volume and cross sectional code increases the already extensive list of uses to which the FRAL may be put.

Since its inception in 2008, the FRAL has been in a constant state of evolution. A few major tasks remain to be completed:

- Integrate all existing aspects of the FRAL into a single program
- Clean the code of unused variables, unneeded comments, and unused subroutines
- Speed runtime for processor intensive processes, particularly the Dynamic Rotation Program

Acknowledgments

The author thanks Nicole Hill of the ESCG Orbital Debris Research and Science Operations (ODRSO) for her efforts to ensure the excellence of the above work. The author also thanks Heather Cowardin, PhD, also with the ODRSO and Sue Lederer, PhD, with the NASA Orbital Debris Program Office, for their expertise that inspired and directed the creation and perfection of the four different plots. The author also extends his thanks to Jiri Silha, Ph.D, (student in the Department of Astronomy at the Faculty of Mathematics, Physics and Informatics Comenius University in Bratislava, Slovakia) for his assistance in the translation and debugging of the volume and mean cross sectional area subroutine. Finally, the author expresses his appreciation for the labor expended by Debra Shoots, with the ODRSO, in editing and formatting this document.

References

[1]"Monthly Number of Objects in Orbit by Object Type" Orbital Debris Quarterly News, Volume 15, Issue 1, Jan. 2011, pp. 10.

[2] Hill, N., "Orbital Measurement Techniques for Hypervelocity Impact Test Fragments" IAC-08-D6.3.10, 2008.

[3]Cowardin, H. "Characterization of Orbital Debris Objects Over Optical Wavelengths via Laboratory Measurements," PhD dissertation, Physics Dept., University of Houston , Houston, TX, 77004, 2011.

[4]Henden, A. and Kaitchuck, R. Astronomical Photometry, Van Nostrand Reinhold Company, New York, 1982 Chaps. 1, 9.

[5]Mulrooney, M. "Optical Phase Functions and Albedos of Orbiting Debris Objects" M.S. Thesis, Rice University, Houston TX, April 1993.

[6]Hapke, B. "An Improved Theoretical Lunar Photometric Function" The Astronomical Journal, Volume 71, Number 5, June 1966.

[7]Johnson, N., Krisko, P. and Liou, J., et al., "NASA's New Breakup Model of EVOLVE 4.0", Advanced Space Research, Volume 28, Issue 9, 2001.

[8]Ojakangas G. "Laboratory Light Curves of Orbital Debris" ODPO Library, JSC, Houston, TX, 2008 (unpublished).

[9]Silha, J., "Documentation of Program Code: dv_silhaHRS.f", ODPO Library, JSC, Houston, TX, 2011 (unpublished).